

Physical model of soil and its implications for landmine detection interference

T. J. Katsube^{*a}, E. Grunsky^a, Y. Das^b, R. DiLabio^a, H. McNairn^c, S. Connell-Madore^a,
E. Gauthier^c, N. Scromeda^a.

^a: Geological Survey of Canada, 601 Booth St., Ottawa, ON K1A 0E8,

^b: Defence R&D Canada Suffield, P.O. 4000, Station Main, Medicine Hat AB, Canada T1A 8K6,

^c: Agriculture and Agri-Food Canada, K. W. Neatby Building, 960 Carling Ave., Ottawa,
ON K1A 0C6, Canada.

ABSTRACT

Many soil physical and chemical properties interfere with landmine detection. Prior knowledge of these properties would improve detection technology selection and increase demining safety and efficiency. Developments in rapid mapping of these properties over wide areas is essential to meet military and economic constraints. Fusion of multiple detection technologies is also essential to overcome detection signal interferences. For these purposes, rapid mapping by use of remote sensing is being tested, starting with electrical conductivity mapping by radar remote sensing. Laboratory induced-polarization (IP) is also being tested to develop techniques to discriminate between electromagnetic signals from metallic particles in landmines and in soil, for regions with detection interference. Key physical models of soil are being developed for fusion of various landmine detection systems and to explain remote sensing responses to soil.

Radar satellite tests carried out over the Canadian Forces Base Suffield (CFBS; Alberta, Canada) in 2004 and 2005 indicated 10 areas for possible high clay content and electrical conductivity. Eight of these were validated by soil maps and Landsat clay images. Two had high organic content with physical characteristics not known at present. Studies on soil with fine-grained iron-oxide powder and on iron with varied degrees of corrosion show that spectral-IP is sensitive to iron or iron-oxides regardless of their state. Soil has layered structure consisting of various grain-size combinations, but its physical characteristics are significantly influenced by whether its clay content is above or below a critical clay content (15 to 25 %). Results of these tests are discussed in this paper with explanations using the soil physical model.

Keywords: Landmine detection, remote sensing, soil electrical conductivity, metal detectors, soil physical model, vehicle trafficability

1. INTRODUCTION

Military and humanitarian demining operations require prior knowledge of soil characteristics for their targeted areas, because various physical and chemical soil properties interfere with their landmine detector systems. Although there are many detection technologies, all are subject to some type of physical and chemical soil property interference². Knowledge of soil property distributions is required to select the most effective landmine detection technology for safe operations in the targeted minefields². For this purpose, rapid soil property mapping methods are being developed by use of remote sensing technology, starting with electrical conductivity (EC) mapping by radar remote sensing⁹, which would be subsequently validated by airborne and surficial geophysical and laboratory testings.

Initial remote sensing results over the Canadian Forces Base Suffield (CFBS: Alberta, Canada), which has dimensions of about 50x50 km, have previously been reported⁹. By visual interpretation of the radar satellite imagery for dry periods over wet periods, 5 areas of similarity were identified, implying areas of high moisture retention¹³. Areas of high moisture retention are expected to have high clay content, implying high electrical conductivity⁹. Validation of these predictions by use of CFBS soil maps indicated that 3 of the 5 similarity areas (SA) had clay containing soil as expected. One had high

*JKatsube@NRCan.gc.ca; phone: 1 613 995 5239; fax: 1 613 943 1286

organic content, also a moisture retaining matter, and one was very sandy, a non-moisture retaining matter which proves difficult to explain. These tests have been followed up by additional radar satellite and Landsat image analyses in 2005, producing interesting results.

In addition to these radar satellite tests, laboratory spectral induced-polarization (IP) tests are being carried out to develop techniques to discriminate between EM signals from metallic particles in landmines and in soil⁶. Also physical models of soil are being developed for laying a basis for fusion of various landmine detection systems and to explain some of the remote sensing responses of soil. In addition, soil iron content mapping by remote sensing has been tested. The purpose of this paper is to document the progress made by these studies and tests.

2. PHYSICAL MODEL OF SOIL

2.1 Soil Forming Process

Soil is an accumulation of loose material of various grain sizes¹⁴. The initial process for soil formation is the disintegration of the bedrock by several weathering processes, such as mechanical and chemical processes. Loosening of tight rocks by temperature changes in warm climates or by volume expansion of freezing pore water in cold climates, and erosion of the rock surfaces by wind, glaciers and water flow are mechanical processes. Chemical processes due to acids from plants can also loosen tight rocks and produce soil. Once a layer of soil is formed on the bedrock surface, additional chemical processes due to acids from the plants or meteoric water movements in the soil can cause alteration of the mineral grains by changing the grain-size or type of minerals. Clays are an example of fine-grained material formed by such processes. There can also be mechanical migration of material, such as clays moving downwards from the surface due to water movement. Following these processes, an initial soil can be removed by wind or water, or additional soil material can be deposited on top of the initial soil due to the same processes transporting material from other sources. This implies that significant vertical changes in the soil column has to be expected due to different degrees of chemical weathering, or soil material deposited from different rock types. Some explanation of this process with illustrations have been discussed previously⁷ and the fundamentals of these processes can be found elsewhere¹⁴.

Vertical movement of water can occur in soil due to temperature variation, evaporation of soil pore water and precipitation. This movement can reach several tens of metres, particularly in tropical climates. This implies that chemicals dissolved by water as deep as the underlying bedrock can be transported to the surface by this vertical water movement. The chemicals that reach the surface can reproduce certain minerals of the bedrock or form new minerals. Certain minerals can even be formed at higher concentration than those in the bedrock. For example, maghemite pebbles at the surface may have a higher iron-oxide content than its bedrock origin⁶.

2.2 Soil Structure

The texture resulting from the soil forming processes is a mixture of clay, silt, sand (fine, medium, coarse) and pebbles¹⁴ with grain sizes in the ranges of $<2\mu\text{m}$, 2 to 63 μm , 0.063 to 2.0 mm and >2.0 mm, respectively. A simplified model of a sand texture is shown in Figure 1 with open spaces between the spherical grains on the upper-right section. The effective porosity (ϕ_E) would be in the range of 40 to 50%, for such a case. The framework grains are unlikely to be spheres, but if angular, they would likely result in lower ϕ_E values. Figure 1 is a useful representation to explain various soil textural effects. If the grain spaces in Figure 1 are filled with silt, then the ϕ_E values would likely be 40 to 50% of that above. Soil is generally considered to have ϕ_E values in the order of 25 to 50 %¹. However, of importance is the point at which clay fills these spaces, which is the critical clay content (CCC,¹⁰). Clay contents at $<CCC$ allows fluid to move through the soil, but at $>CCC$ the fluid permeability would decrease rapidly and many soil physical property changes can occur. The CCC is estimated to be in the order of 15 to 25 %⁵. The effect of clay is very different from the other grains because it has a flaky texture which is unlike the other granular textures. Decayed organic material may also have an effect similar to clay.

2.3 Distribution of Minerals that Affect the Soil Physical Properties

Magnetic susceptibility (MS), electrical conductivity (EC) or resistivity (ER) and water retention are all important soil characteristics. The source of the ferro-magnetic minerals in soil is the local bedrock or transported from elsewhere. When bedrock containing ferro-magnetic minerals (e.g., magnetite) disintegrate due to the weathering they will remain in the resulting soil. In the case of vertical movement of water in the soil column, new ferro-magnetic minerals (e.g., hematite

and maghemite) can be produced and deposited at the surface. These minerals can be relatively large in grain sizes, such as 0.25 to 2 mm (medium to coarse sand sizes) or >2.0 mm (pebble sizes) and may have very high MS values, as previously indicated⁶. Transported material, from other areas and deposited on the soil formed from the local bedrock, can also contain significant amounts of ferro-magnetic minerals, such as magnetite, sulphides (e.g., pyrrhotite). These materials can be a result of eroded bedrock containing ferro-magnetic minerals, iron-rich ore deposits or sulphide-rich veins (e.g., pyrite, pyrrhotite). A result of these processes is the replacement of the large mineral grains in Figure 1 with these iron-oxide grains.

The main source of high soil EC or low ER is saline water or clays, excluding kaolinite (Table 1). Clay particles are usually interconnected, unless they are interrupted by the framework grains (Fig. 1). Metallic minerals or particles are not necessarily significant sources of EC, as they usually lack inter-connectivity. Soil water ERs are usually in the range of 0.05 to 100 Ωm ^{11, 7}. The soil water ER values are related to the bedrock type¹¹ and the climate. Areas with considerable evaporation can result in high salinity water at the surface and reduce the soil ER values.

Interconnected clay layers can be a major source of soil high EC or low ER (Table 1). Clay ER values are related to their cation exchange capacity (CEC) and surface area (A), with montmorillonite showing some of the lowest ER values (Table 1) and highest CEC and A values (Table 2). Similarly, kaolinite shows one of the highest ER and lowest CEC and A values. Clay is a result of chemical alteration of rock or soil-forming minerals, and is due to various weathering and mechanical transport processes, as previously indicated. It is distributed throughout a soil column, often forming layers of different concentrations.

Figure 1: Model of a framework supported texture with a varying degree of clay matrix filling the intergranular pore spaces⁵.

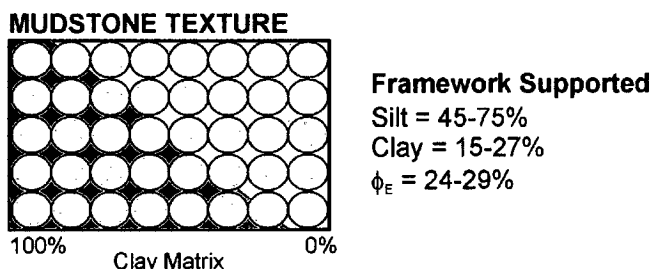


Table 1: Electrical conductivity (EC) characteristics of some major soils and clays¹⁵.

Material	Soils and Clays	Electrical Resistivity (Ωm)	Electrical Conductivity (mS/m)
Soil Types	Clay (general term)	1 - 100	10 - 1000
	Loam	4 - 40	25 - 250
	Top Soil	40 - 200	5 - 25
	Clay-rich Soil	100 - 400	2.5 - 10
	Sandy Soil	400 - 4000	0.25 - 2.5
	Loose Sands	1000 - 10 ⁵	0.01 - 1
Clay Type	Kaolinite	50 - 5000	0.2 - 20
	Montmorillonite	4 - 15	67 - 250

Table 2: Cation exchange capacity (CEC) and surface areas (A) of some common clay minerals³.

Clay Minerals	CEC (me/100 g)	Surface Area (m^2/g)
Vermiculite	100 - 150	600 - 800
Montmorillonite	80 - 120	600 - 800
Illite	10 - 40	65 - 100
Chlorite	10 - 40	25 - 40
Kaolinite	3 - 15	7 - 30

2.4 Layered Structure of Soil

Soil is an accumulation of loose material with a layered structure consisting of various grain-size combinations¹⁴. This is a result of the various soil-forming and secondary alteration processes, previously described. A schematic diagram of a landscape section, consisting of fresh bedrock overlain with layers of various degrees of weathered rock and soil is shown in Figure 2. Soil resulting from weathered bedrock of ultramafic and felsic type are shown in the left-hand side of Figure 3. In this case, the former is a basic rock rich in ferro-magnetic minerals and the latter is an acidic rock poor in these minerals. As shown in the diagram, soil above the basic or acidic bedrocks are rich or poor in ferro-magnetic minerals, respectively. The upper section of the right-hand side of Figure 3 illustrates a case where a ferro-magnetic rich soil has been transported and deposited above a ferro-magnetic poor soil. The lower section illustrates a case where ferro-magnetic minerals (e.g., magnetite) in a bedrock poor in such minerals has dissolved by the vertical movement of ground water and been transported to the surface to produce a new ferro-magnetic mineral (e.g., maghemite). In this case, the new ferro-magnetic mineral can be of higher iron concentration than that in the bedrock. This section also illustrates the case where relatively large pebble-size (>2 mm) concretions of ferro-magnetic minerals have formed at the surface. The layers immediately below that layer contain smaller grains of the same new mineral that have not yet grown to the pebble-sized grains at the surface. These descriptions are a repetition of those in a previous publication⁷.

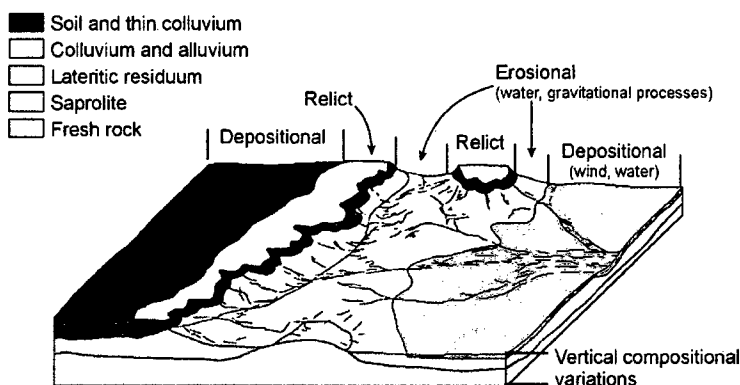


Figure 2: Landscape model illustrating fresh bedrock overlain with layered structure of soil, consisting of various degrees of weathered rock and soil transported by different processes⁷.

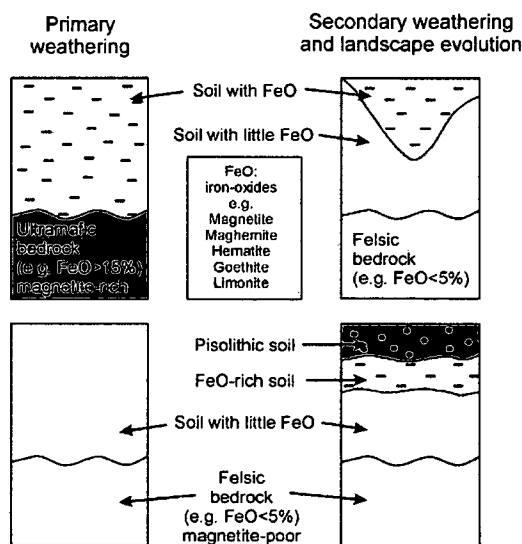


Figure 3: Layered structure of soil⁷. [Left-hand side] Soil resulting from weathered bedrock of ultramafic (upper) and felsic (lower) types. [Upper-Right] An illustration of a case where a ferro-magnetic rich soil has been transported and deposited above a ferro-magnetic poor soil. [Lower-right] Illustration of a case where ferro-magnetic minerals (e.g., magnetite) in a bedrock poor in such minerals has dissolved by the vertical movement of ground water and has been transported to the surface to produce a new ferro-magnetic mineral (e.g., maghemite).

3. MAPPING STRATEGY

Since soil EC interferes with a number of widely used detector systems², such as metal detectors and ground penetrating radar systems, we are developing a rapid mapping technique for EC using radar remote sensing. Soil metallic minerals can also interfere with the metal detector signals, and some of their distribution may be mapped by Landsat TM band ratio 3/2 as shown in Figure 4. In this paper, however, we will focus on EC mapping due to soil moisture. In principle, areas of moderate to high soil moisture content with little change over time are associated with high moisture retention due to higher clay content¹³, suggesting higher EC⁸. Based on this principle, initial EC mapping tests were carried out at the Canadian Forces Base Suffield (CFBS; Alberta, Canada), by satellite remote sensing for prediction of soil moisture change using RADARSAT backscatter similarity/change characteristics⁹. As a result, 5 radar backscatter Similarity Areas (SA), numbers M1 to M5, were visually identified (Fig. 5). The dimensions of these areas are about 2x2 km, 2x4 km and 4x4 km for M1, M2 and M3, respectively, and about 5x13 km and 4x4 km for M4 and M5, respectively. Validation of these results by soil survey and military trafficability maps¹² for the base indicated that two SA's (M1 and M5) were clearly related to clay in the soil. Another two (M2 and M3) were related to high organic content (chernozem and rego gleysol) in the soil, with the latter being saline. Organic matter also has high water retention characteristics. According to the soil map, SA-M4 is a very sandy area with poor trafficability characteristics, which contradicts the high water retention principle. This RADARSAT has a C-Band sensor (frequency of 5.3 GHz or 5.6 cm wavelength). The data were acquired in an ascending orbit, in Standard modes S1 and S2 at incidence angles of 20 to 27° and 24 to 31°, respectively. The nominal spatial resolution of Standard mode data is 25 m. The daily precipitation data leading up to the date of acquisition and other details have been published elsewhere⁹. The Surface Geological Map of Alberta also shows that SA-M4 is a very sandy area. In a separate study, the 2006 MDA EarthSat image shows that a saline area (alkaline) extends to about 5 km east beyond the boundaries of SA-M3.

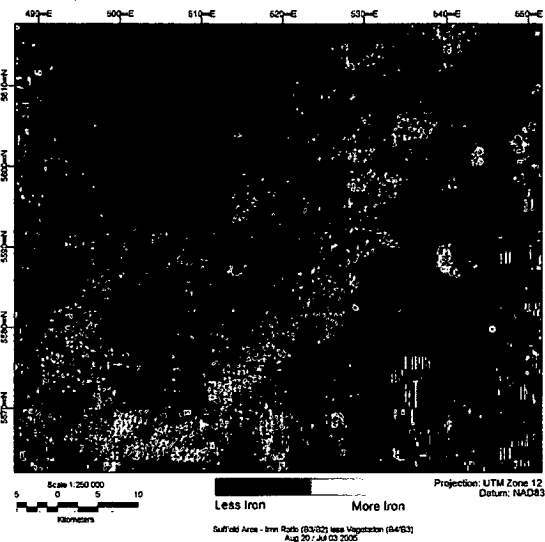


Figure 4: Iron-oxide distribution in the Canadian Forces Base Suffield (CFBS; Alberta, Canada) mapped by Landsat imagery (TM band ratio 3/2, July 27, 1999). The areas with increased brightness represent increased iron-oxide content in the soil.

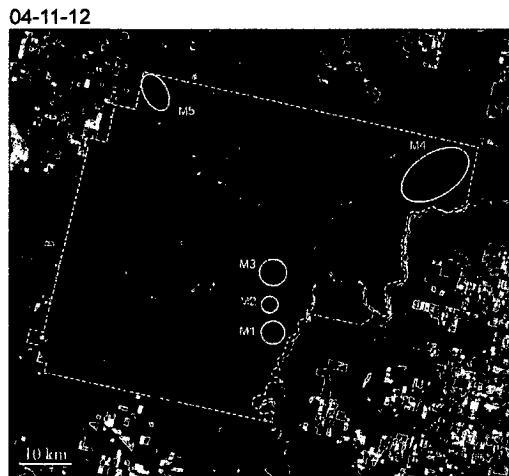


Figure 5: RADARSAT backscatter images for November 12, 2004 over the CFBS with bright areas highlighted (M1 to M5), identifying areas having high soil moisture retention characteristics⁹.

Although the CFBS soil map did not show any indication of clay for SA-M4, the Landsat TM band ratio 5/7 (July 26, 1999) for clay distribution shows an increased clay content for that area (Fig. 6). However, the responses are not as pronounced as those associated with some of the other SAs. For example, the Landsat response for the M1 is very pronounced but for a very limited area (difficult to see in Fig. 6). The response for M5 is characterized by scattered and extremely small areas with intense clay responses. It is interesting that M3, which was considered to be a response to organic material⁹, shows a considerably pronounced clay response in the Landsat image. This implies we have evidence that 4 of the 5 SAs are related to an increased clay content. The reason that M4 showed a RADARSAT response that was not identified in the soil map is likely because the clay content was low. There is a critical clay content (CCC) of about 15 to 25 % under which it has little effect on many physical characteristics of the geological material and above which it dominates those characteristics^{5,10}, as explained in Figure 1. The fact that the trafficability of that area was poor suggests that its clay content may have been below the CCC. One question still remains, however, which is why some clay rich areas identified in the soil map and in the Landsat image did not produce noticeable responses in the 2004 RADARSAT images. The bright area in Figure 6 south of M4 is one of them.

The 2005 RADARSAT image for August 20 (dry period) following July 3 (wet period) is displayed in Figure 7. The daily precipitation leading up to this acquisition is listed in Table 3. The bright areas represent higher moisture retention than those around them. All SAs (M1 to M5) of the 2004 RADARSAT backscatter image are repeated in this image. The backscatter signals in the northwest section covers a much wider area than that of M5, likely due to effects other than clay, such as soil disturbances caused by industrial activities that did not exist in the fall 2004 acquisition. The 2005 RADARSAT image identifies new SAs, N1 to N5, with varied backscatter signal intensity. SA-N1 has relatively high intensity, but the CFBS soil map indicates that it is in a sandy area similar to M4, likely implying a clay content below the CCC. The Surface Geological Map of Alberta also shows that SA-N1 is a very sandy area. SAs-N2, N4 and N5 show high backscatter signal responses. Although limited in size, they are related to Landsat clay responses. The area covered by N3 appears reasonably large. SAs-N4 and N5 appear to represent clusters of multiple small areas with strong clay responses. The backscatter signal intensity is low for SA-N3 with little indication of clay by Landsat, but an indication of organic material existence by the soil map. The results of this study suggests that the SAs of 2004 (M1 to M5) and 2005 (N1 to N5) have been validated reasonably well by the combination of the CFBS soil map and the Landsat clay image. However, these conclusions should be validated further by airborne and ground electromagnetic (EM) surveys and laboratory tests.

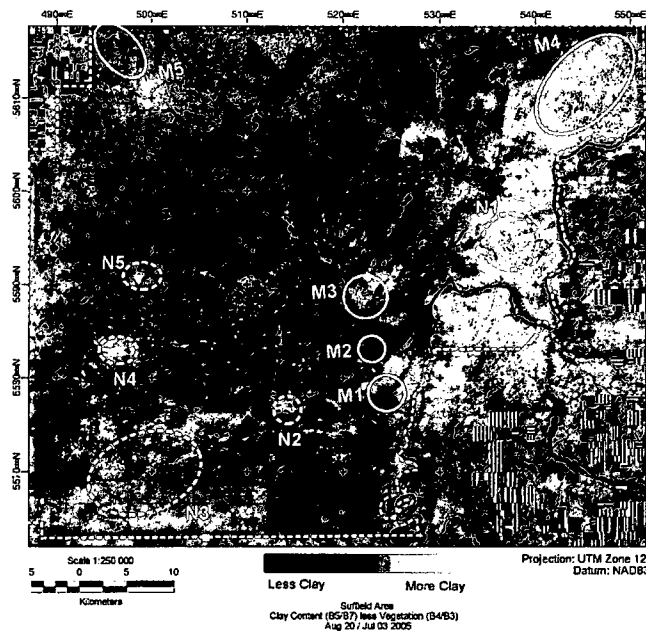


Figure 6: Landsat (Band 5 and 7, July 26, 1999) image showing clay distribution over the CFBS. The areas with increased brightness represent increased clay content in the soil.

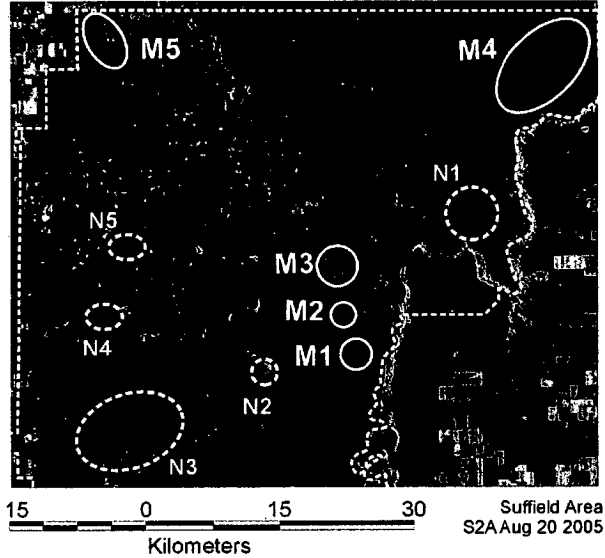


Figure 7: RADARSAT backscatter images for August 20, 2005 (dry period) over the CFBS, repeating the SAs of 2004⁹ and identifying 5 new SAs (N1 to N5).

Table 3: Weather data for the Canadian Forces Base Suffield between June 09 and August 20, 2005 (Data provided by the weather station on the base).

Date	BP	t (UTC)	T (°C) Min/Max	Precipitation (rain in mm) and Days Prior to Acquisition						
				6	5	4	3	2	1	0
Jun. 09	S2	00:59:55	8/15	6.0	3.1	3.5	23.3	13.4	tr	3.5
Jul. 03	S2	00:59:50	9/22	15.9	19.2	0.4	0	3.2	6.0	
Aug. 20	S2	00:59:45	7/30	tr	4.1	0.4	4.3	0.2	0	

Date = Date of RADARSAT C-Band Acquisition in 2005.

BP = Beam Position for the Standard Beam Mode.

t = Time of RADARSAT Acquisition.

UTC = Coordinated Universal Time or Greenwich Mean Time.

T = Temperature.

Min/Max= Minimum and Maximum temperatures.

tr = Trace.

S2 = Incidental Angle of 24-31 degrees (Ascending) and a resolution of 25 m.

4. LABORATORY SPECTRAL INDUCED POLARIZATION (IP) TESTS

A spectral induced polarization (IP) study⁶ was carried out on a sample of Cambodian soil salted with various concentrations of fine-grained iron-oxide powder. The purpose was to determine the spectral-IP characteristics of the iron-oxides in soil, and whether they may be used to distinguish iron-oxides in soil from the small metallic particles in landmines, in regions of significant landmine detection interference. Spectral-IP characteristics, in this case, implies the complex electrical resistivity characteristics over a frequency range of 1.0 to 10⁶ Hz. The difference between metallic electrical conductors in a landmine and in soil is that the former is cased in insulated material resulting in constant EC, and the latter is usually in contact with moisture forming electrochemical double layers on its surface. This double layer will act like a capacitor in an electrical circuit. If an eddy or galvanic current passes through the metallic particle into the soil, the capacitive effect of the double layer would cause the EC to vary with frequency, a characteristic that could distinguish the iron-oxides or ferromagnetic minerals from the landmine detonators. Further details of this theory have been previously discussed⁶.

The expected effect that conductive mineral content has on soil spectral-IP characteristics are shown in Figures 8a to 8c⁶. The ρ^+ and $\Delta\rho^+$ in the figures are the complex resistivity amplitude and complex resistivity gradient, respectively, where $\Delta\rho^+$ is determined by

$$\Delta\rho^+ = (\rho^+_i - \rho^+_{i+1})/\rho^+_i, \quad (1)$$

and where i and $i+1$ represent a specific frequency and its adjacent frequency (e.g., 10 and 30 Hz or 300 and 1000 Hz) at which these measurements were taken. Figure 8b shows that although $\Delta\rho^+$ varies considerably with frequency, the frequency at which the $\Delta\rho^+$ shows the maximum value varies little. However, its amplitude increases with increased conductive metallic particle content (20 to 60 vol.%). This model is explained in a previous publication⁴ which uses a permittivity (ϵ_M) value of 10^{-6} F/m for the conductive mineral surfaces. The effect of grain size on the frequency at which the $\Delta\rho^+$ shows a maximum value is shown in Figure 8c, indicating that the frequency increases with decreased grain-size. This is based on the assumption that the volume of the conductive metallic particle content is 40 % and the grain size varies from 1 to 100^{th} of what it was in Figure 8b. In this case, the intrinsic surface capacitance of the conductive mineral does not change but the capacitance of the entire mineralization decreases with decreased grain size because the number of grains that an electrical current traverses increases, resulting in an increased number of series capacitors⁶.

Results of the spectral-IP characteristics for the Cambodian soil salted with fine-grained magnetite varying over a range of 5 to 20 wt% are shown in Figures 9a and 9b. Following this, the bulk soil was salted with 10 wt% of fine-grained magnetite (<0.062 mm), coarse-grained magnetite (0.062 to 0.71 mm), small magnetic-pebbles (3 to 6 mm) and large magnetic-pebbles (5 to 11 mm). Results for these spectral-IP measurements are shown in Figure 9c. The iron-oxide mineral (maghemite) content of the magnetic pebbles is estimated to be in the order of 30 to 70 volume%⁶. The spectral-IP characteristics for the salted Cambodian sample (Figs 9a, b) show considerable variation with the magnetite powder content (0 to 20 %) and have considerable similarities with those of the theoretical curves in Figure 8, such as the $\Delta\rho^+$ -f curves in Figures 9b and 8b. Similar trends are seen for the bulk Cambodian sample salted with 10 wt. % of magnetite of varied grain-sizes, as shown in Figure 9c and 8c. These consistencies suggest that the theoretical basis for the measured spectral-IP characteristics are relatively well understood. These results have indicated that spectral-IP characteristics are sensitive to relatively small changes in iron-oxide content, such as 0, 2, 5 and 10 %⁶. The question now is whether the same trends can be seen if the iron-oxide grains are corroded.

In order to test the effect of corrosion, the complex impedance (Z^*) of soil containing iron balls with varied degrees of corrosion were tested under routine petrophysical laboratory conditions⁴. First, the soil in moist condition was placed into a circular sample holder and the Z^* measured. Then an iron ball (about 1.5 cm in diameter) with a non-corroded shiny surface was inserted into the soil of the sample holder and the Z^* measured. The iron ball was left in the moist soil for up to 28 days with periodic Z^* measurements. After the 28th day, the ball had a layer of corrosion, about 2 to 5 mm in thickness. Photographs of the ball when fresh and after the 28 day period are shown in Figure 10. The Z^* is expressed by

$$Z^* = Z' - jZ'', \quad (2)$$

where Z' and Z'' are the real and imaginary impedances⁴. The iron ball in soil can be represented by the equivalent circuit displayed in Figure 11. The $C_M\omega^a$, R_M , R_p and C_D are the frequency dependent capacitance of the electrochemical double layer on the iron ball, the soil resistance between the ball and the electrodes of the sample-holder, resistivity of the soil between the ball and the surrounding wall of the sample holder, and the soil sample capacitance due to its dielectric constant. The symbol a is represented by α_M in the diagram. Explanation of the other symbols are given the caption of Figure 11.

The results of the Z^* measurements represented by Z'' for one of the balls are shown in Figure 12. The continuous increase of Z'' with time at the higher frequencies ($>10^3$ Hz) is due to the effects of the soil dielectric constant and the soil grain surface adsorbed water layers^{8, 9}. The increased Z'' values between the frequency range of 30 to 10^4 Hz is due to the capacitance (C_M) of the electrochemical double layer on the iron ball surface. These results suggest that the spectral-IP characteristics are sensitive to all stages of corrosion of the iron ball.

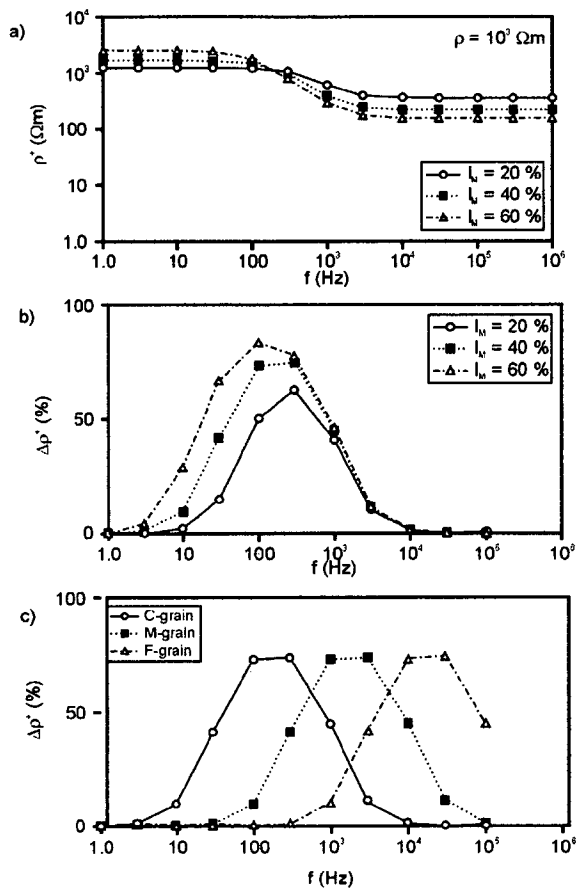


Figure 8: Theoretical curve⁶ for the spectral-IP characteristics of (a) & (b) varied metallic mineral concentration ($I_M = 20$ to 60 volume %) and (c) grain sizes (C: coarse, M: medium and F: fine). The ρ^* , $\Delta\rho^*$ and f are the amplitude of the complex resistivity, gradient of the complex resistivity and the frequency, respectively.

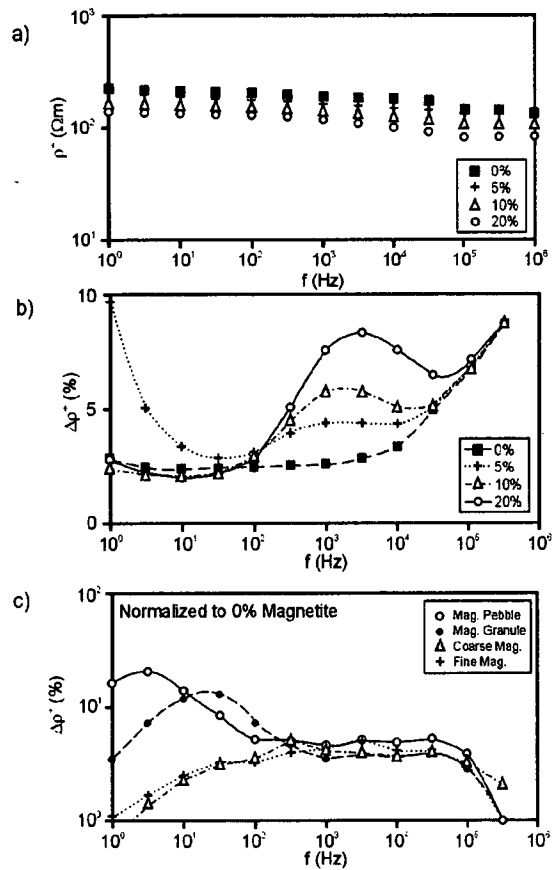


Figure 9: Spectral-IP characteristics of the bulk Cambodian soil sample, salted with fine grained magnetite powder in the range of 0 to 20% for (a) the ρ^* - f curves, (b) the $\Delta\rho^*$ - f curves, and (c) the $\Delta\rho^*$ - f curves for the bulk Cambodian sample salted with 10 wt. % of magnetite of varied grain sizes, ranging from fine-grained powder (<0.062 mm), coarse-grained powder (0.062 to 0.71 mm), small pebbles (3 to 6 mm) to large pebbles (5 to 10.3 mm). The $\Delta\rho^*$ - f curves for c) have been normalized to the salted magnetite content of 0 wt %.

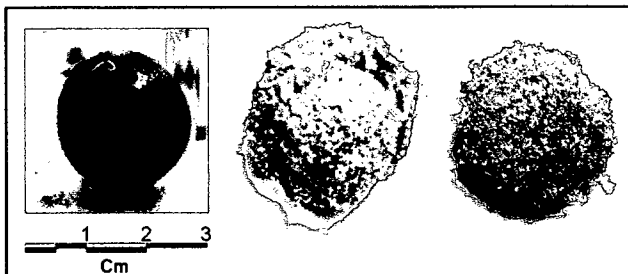


Figure 10: Photographs of one of the iron balls (about 1.5 cm in diameter) at varied degrees of corrosion, increasing from left to right.

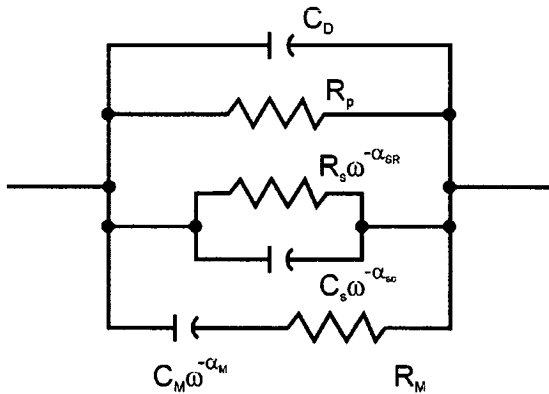


Figure 11: Equivalent circuit of an anisotropic mineralized rock⁴. The C_D is the capacitance due to the dielectric characteristics of the rock, R_p is the resistance to the electrical current flowing through the pores of the non-mineralized layer, and $R_s \omega^{-\alpha_{SR}}$ and $C_s \omega^{-\alpha_{\omega}}$ are the frequency dependent resistance and capacitance of the pore surfaces in the non-mineralized layer, where a and b are coefficients and ω is the angular frequency. The R_M and $C_M \omega^{-\alpha_M}$ are the resistance and frequency dependent capacitance of the mineralized layers, where C is a coefficient. [$a : \alpha_{SR}$; $b : \alpha_{SC}$; $c : \alpha_M$]

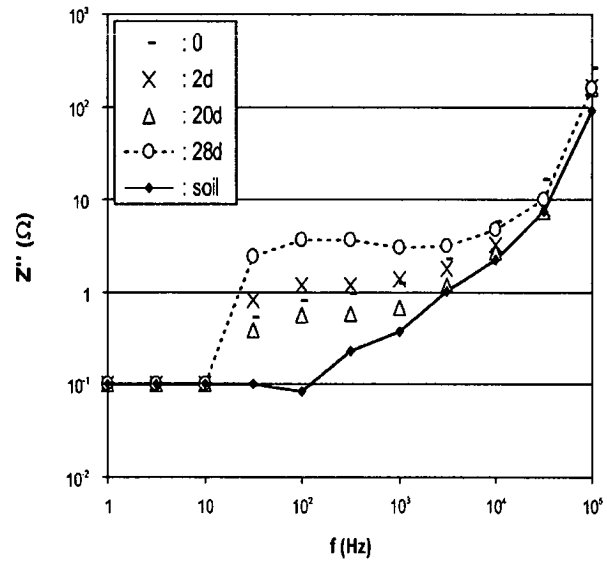


Figure 12: Imaginary impedance (Z'') versus frequency (f) for an iron ball (about 1.5 cm in diameter) buried in soil at various stages of corrosion.

5. DISCUSSION AND CONCLUSIONS

Soil is an accumulation of loose material of various grain sizes and is formed by disintegration of bedrock by several weathering processes, such as mechanical and chemical processes¹⁴. The resulting texture is a mixture of clay, silt, sand (fine, medium, coarse) and pebbles with grain sizes in the ranges of $<2\mu\text{m}$, 2 to 63 μm , 0.063 to 2.0 mm and >2.0 mm, respectively. Soil is also an accumulation of loose material with layered structure consisting of various grain-size combinations. The key point is whether the clay content exceeds or is below the critical clay content (CCC) which is about 15 to 25%. The CCC is the point at which clay fills the spaces between the framework silt and sand grains. The physical properties of soil, such as permeability, electrical conductivity (EC) and sonic velocity, vary considerably depending on whether the clay content is above or below the CCC^{10,5}. Decayed organic material may also have an effect similar to clay. Iron-oxides would likely replace some of the framework grains, but not necessarily contribute to EC unless they are interconnected.

Rapid EC mapping techniques are being developed by use of radar remote sensing, since soil EC interferes with a number of widely used detector systems, such as metal detectors and ground penetrating radar². In principle, areas of moderate to high soil moisture content with little change in time are associated with high moisture retention due to higher clay content¹³, suggesting higher EC⁸. Soil metallic minerals can also interfere with the metal detector signals and their distribution may be mapped by Landsat TM band ratios. This paper, however, focuses on the use of moisture retention for mapping EC, since there are still unknown factors related to metallic mineral mapping by Landsat.

EC mapping tests were carried out in 2004⁹ and 2005 at the CFBS using RADARSAT. As a result, 10 radar backscatter Similarity Areas (SA), numbers M1 to M5 and N1 to N5, were visually identified with dimensions in the order of 2x2 km to 5x13 km. Validation by soil survey maps¹² and Landsat clay response images suggested that 6 of these SA's were related to high clay content in the soil, two were related to low clay content and the remaining two were related to high organic (chernozem and rego gleysol) content, which also has high water retention characteristics. The 6 SA's with high clay content are considered to represent high soil EC. The two SA's with low clay content are considered to have a clay content below the CCC and likely lower soil EC. The SA's with high organic content could be related to higher soil EC, but it is not clear at this time. This implies, however, that soil maps and Landsat images indicate that SA's identified by RADARSAT backscatter signal images can provide significant information on the possible areas of high soil EC. That is, all SAs have been validated reasonably well by the combination of the CFBS soil map and the Landsat clay image. However, these conclusions should be validated further by airborne and ground electromagnetic (EM) surveys and laboratory tests.

Spectral-IP studies are in progress to determine if the technique can be used to distinguish iron-oxides in soil from the small metallic particles in landmines, for regions of significant landmine detection interference. Spectral-IP characteristics, in this case, implies complex electrical resistivity characteristics over a frequency range of 1.0 to 10⁶ Hz. Previous studies⁶, on Cambodian soil salted with various concentrations of fine-grained iron-oxide powder, showed promising results. The question now is whether similar results can be seen if corrosion is involved. For this purpose, complex impedance (Z^*) of soil containing iron balls (about 1.5 cm in diameter) with varied degrees of corrosion have been tested. Balls with maximum degrees of corrosion had corrosion layers of about 2 to 5 mm in thickness. Significant differences in the imaginary impedance (Z'') due to the ball for all degrees of corrosion have been seen in the frequency range of 30 to 10⁴ Hz. This is due to the capacitance (C_M) of the electrochemical double layer on the iron ball surface. These results suggest that the spectral-IP characteristics are sensitive to all stages of corrosion of the iron balls, likely implying corroded iron-oxides of all grain-sizes. However, further tests are recommended to confirm this conclusion.

ACKNOWLEDGMENTS

The authors acknowledge the contribution by Mr. T. Hansen (Weather Station on the Canadian Forces Base Suffield, Alberta, Canada) for supplying the precipitation and temperature data for the Base prior to the RADARSAT acquisitions. The authors also acknowledge the comments and advice provided by Dr. S. Wolfe and Dr. L. Dyke of the Geological Survey of Canada (GSC-Ottawa). The iron balls were provided by Mr. P. Newcombe (Canada Center for Mineral and Energy Technology, Ottawa, Canada). The authors acknowledge the critical review of this paper by J. Carson (GSC-Ottawa).

REFERENCES

1. Buckman, H. O. and Brady, N. C., *The Nature and Properties of Soil*, 7th Edition; The Macmillan Company, New York, Toronto, 653 pp, 1970.
2. Das, Y., McFee, J. E., Russell, K., Cross, G., and Katsube, T. J., *Soil information requirements for humanitarian demining*; The case for a soil properties data base: Detection and Remediation Technologies for Minelike Targets, VIII, (ed: R. S. Harmon, J. H. Holloway, Jr., J. T. Broach), The Proceedings of SPIE (The International Society for Optical Engineering), Volume 5089 (2003.), 1146-1157, 2003.
3. Grim, R.E., *Clay Mineralogy*, 2nd Edition; McGraw Hill Book Company, New York, 596 pp, 1968.
4. Katsube, T. J., *An analytical procedure for determining spectral induced polarization characteristics of anisotropic rocks, Yellowknife mining district, Northwest Territories*: Geological Survey of Canada Current Research, 2001-E3; 11 p, 2001.
5. Katsube, T. J., Dallimore, S. R., Uchida, T., Jenner, K. A., Collett, T.S., and Connell, S., *Petrophysical environment of sediments hosting gas-hydrate, JAPEX/JNOC/GSC Mallik 2L-38 gas hydrate research well: in Scientific Results from JAPEX/JNOC/GSC Mallik 2L-38 Gas Hydrate Research Well, Mackenzie Delta, North*

- West Territories, Canada:* (ed.) S. R. Dallimore, T. Uchida, and T.S. Collett; Geological Survey of Canada, Bulletin 544, 109-124, 1999.
6. Katsube, T. J., Klassen, R. A., Das, Y., Benn, K., Best, M. E., and Ernst, R., *Electromagnetic characteristics of Cambodian soil: Implications for landmine detection in soil containing ferromagnetic minerals:* The Proceedings of SPIE (The International Society for Optical Engineering), Detection and Remediation Technologies for Minelike Targets VII (ed: J. T. Broach, R. S. Heramon, G. J. Dobeck) SPIE Vol. 4742 (2002), 821-835, 2002.
 7. Katsube, T. J., Klassen, R. A., Das, Y., Ernst, R., Calvert, T., Cross, G., Hunter, J., K., Best, M. E., DiLabio, R., and Connell, S., *Prediction and validation of soil electromagnetic characteristics for application in landmine detection: Detection and Remediation Technologies for Minelike Targets, VIII,* (ed: R. S. Harmon, J. H. Holloway, Jr., J. T. Broach), The Proceedings of SPIE (The International Society for Optical Engineering), Volume 5089 (2003.), 1219-1230, 2003.
 8. Katsube, T. J., Keating, P. K., H. McNairn, Das, Y., DiLabio, R., Singhroy, V., Connell-Madore, S., Best, M.E., Hunter, J., Klassen, R. and Dyke, L., *Soil moisture and electrical conductivity prediction and their implication for landmine detection technologies:* In Proceedings of SPIE (The International Society for Optical Engineering), Vol 5415, Detection and Remediation Technologies for Mines and Minelike Targets IX (ed: R.S. Harmon, J.T. Broach and J.H. Holloway, Jr.), p. 691-704, 2004.
 9. Katsube, T. J., McNairn, H., Das, Y., Gauthier, E., Holt, R. M., Singhroy, V., DiLabio, R., Connell-Madore, S., and Dyke, L., *Rapid mapping of soil electrical conductivity by remote sensing: implication for landmine detection and vehicle mobility:* In Proceedings of SPIE (The International Society for Optical Engineering), Vol 5794, Detection and Remediation Technologies for Mines and Minelike Targets X (ed: R. S. Harmon, J. T. Broach and J. H. Holloway, Jr.), p. 144-156, 2005.
 10. Katsube, T. J., and Connell-Madore, S., *Inter-connecting or flow pore characteristics of unconsolidated and cemented shales: implication for fluid flow,* in preparation.
 11. Keller, G. V., *Electrical properties of rocks and minerals:* in Handbook of Physical Properties of Rocks, Vol. I (ed. Carmichael, R.S.), CRC Press, Inc., Florida, 217-293, 1982.
 12. Kjearsgaard, A.A., *Soils of the Suffield Military Reserve:* Alberta Institute of Pedology, Report No. M-73-9, 48 p., 5 Maps, 1973.
 13. McNairn, H., Boisvert, J.B., and Pultz, T. J., *Active microwave remote sensing methods; In Methods of Soil Analysis: Part 4 - Physical Methods (Third Edition),* J.H. Dane and G.C. Topp, Editors. Soil Science Society of America, Inc, Madison, Wisconsin, USA, 1692 pp , 2002.
 14. Mitchell, J. K., *Fundamentals of Soil Behaviour Second Edition:* published by John Wiley & Sons, Inc., New York, Chichester, Brisbane, Singapore, 437 pp , 1993.
 15. Walker, J. W., Hulse, W. H., and Fcart, D. W., *Observations of the electrical conductivity of the tropical soils of Western Puerto Rico:* Geological Society of America Bulletin (84), 1743-1752, 1973.

525767
CA027895